Inorg. Chem. **2009**, *48*, 2932−2943

Copper(II) Complexes of L-Arginine as Netropsin Mimics Showing DNA Cleavage Activity in Red Light

Ashis K. Patra,[†] Tuhin Bhowmick,[‡] Sovan Roy,[†] Suryanarayanarao Ramakumar,[‡] and Akhil R. Chakravarty*,[†]

Department of Inorganic and Physical Chemistry and Bioinformatics Center, Department of Physics, Indian Institute of Science, Bangalore 560 012, India

Received September 10, 2008

Copper(II) complexes $[Cu(L\text{-arg})_2](NO_3)_2$ (**1**) and [Cu(L-arg)(B)Cl]Cl (**2**−**5**), where B is a heterocyclic base, namely, 2,2′-bipyridine (bpy, **2**), 1,10-phenanthroline (phen, **3**), dipyrido[3,2-d:2′,3′-f]quinoxaline (dpq, **4**), and dipyrido[3,2-a:2′,3′-c]phenazine (dppz, **5**), are prepared and their DNA binding and photoinduced DNA cleavage activity studied. Ternary complex **3**, structurally characterized using X-ray crystallography, shows a square-pyramidal (4 + 1) coordination geometry in which the N,O-donor L-arginine and N,N-donor 1,10-phenanthroline form the basal plane with one chloride at the elongated axial site. The complex has a pendant cationic guanidinium moiety. The one-electron paramagnetic complexes display a metal-centered d−d band in the range of 590−690 nm in aqueous DMF. They show quasireversible cyclic voltammetric response due to the Cu(II)/Cu(I) couple in the range of −0.1 to −0.3 V versus a saturated calomel electrode in a DMF-Tris HCl buffer (pH 7.2). The DNA binding propensity of the complexes is studied using various techniques. Copper(II) bis-arginate **1** mimics the minor groove binder netropsin by showing preferential binding to the AT-rich sequence of double-strand (ds) DNA. DNA binding study using calf thymus DNA gives an order: **5** (L-arg-dppz) ≥ **1** (bis-L-arg) > **4** (L-arg-dpq) > **3** (L-arg-phen) ≫ **2** (L-arg-bpy). Molecular docking calculations reveal that the complexes bind through extensive hydrogen bonding and electrostatic interactions with ds-DNA. The complexes cleave supercoiled pUC19 DNA in the presence of 3-mercaptopropionic acid as a reducing agent forming hydroxyl (•OH) radicals. The complexes show oxidative photoinduced DNA cleavage activity in UV-A light of 365 nm and red light of 647.1 nm (Ar−Kr mixed-gas-ion laser) in a metal-assisted photoexcitation process forming singlet oxygen ($^1O_2$) species in a type-II pathway. All of the complexes, barring complex **2**, show efficient DNA photocleavage activity. Complexes **4** and **5** exhibit significant double-strand breaks of DNA in red light of 647.1 nm due to the presence of two photosensitizers, namely, L-arginine and dpq or dppz in the molecules.

Introduction

Metal-based pseudonucleases are of current interest in nucleic acid chemistry for their diverse applications like footprinting, sequence-specific binding to nucleic acids, and as new structural probes and therapeutic agents.[1−10] Metal complexes that selectively bind and cleave DNA under physiological conditions in the absence of any external reagents but do so on irradiation with visible light are of particular interest for their potential phototherapeutic ap-

* To whom correspondence should be addressed. Fax: +91-80-23600683. E-mail: arc@ipc.iisc.ernet.in.
† Department of Inorganic and Physical Chemistry.
‡ Bioinformatics Center, Department of Physics.

(1) Sigman, D. S. *Acc. Chem. Res.* **1986**, *19*, 180. Sigman, D. S.; Bruice, T. W.; Mazumder, A.; Sutton, C. L. *Acc. Chem. Res.* **1993**, *26*, 98. Sigman, D. S.; Mazumder, A.; Perrin, D. M. *Chem. Rev.* **1993**, *93*, 2295.
(2) Boerner, L. K. J.; Zaleski, J. M. *Curr. Opin. Chem. Biol.* **2005**, *9*, 135.
(3) Erkkila, K. E.; Odom, D. T.; Barton, J. K. *Chem. Rev.* **1999**, *99*, 2777.
(4) Chifotides, H. T.; Dunbar, K. R. *Acc. Chem. Res.* **2005**, *38*, 146.
(5) Pogozelski, W. K.; Tullius, T. D. *Chem. Rev.* **1998**, *98*, 1089.
(6) Burrows, C. J.; Muller, J. G. *Chem. Rev.* **1998**, *98*, 1109.
(7) McMillin, D. R.; McNett, K. M. *Chem. Rev.* **1998**, *98*, 1201.
(8) Cowan, J. A. *Curr. Opin. Chem. Biol.* **2001**, *5*, 634. Hegg, E. L.; Burstyn, J. N. *Coord. Chem. Rev.* **1998**, *173*, 133. Wolkenberg, S. E.; Boger, D. L. *Chem. Rev.* **2002**, *102*, 2477. Franklin, S. J. *Curr. Opin. Chem. Biol.* **2001**, *5*, 201. Liu, C.; Wang, M.; Zhang, T.; Sun, H. *Coord. Chem. Rev.* **2004**, *248*, 147.
(9) Pratviel, G.; Bernadou, J.; Meunier, B. *Angew. Chem., Int. Ed. Engl.* **1995**, *34*, 746.
(10) Reedijk, J. *J. Inorg. Biochem.* **2001**, *86*, 89.

10.1021/ic8017425 CCC: $40.75
Published on Web 03/02/2009

plications that include the photodynamic therapy (PDT) of cancer.[11−20] PDT has emerged as a noninvasive method for the treatment of cancer by selective photoactivation of the drug as a photosensitizer at the cancer cells using visible radiation of 630−800 nm wavelength, leaving the healthy cells unaffected. Photofrin, the currently used hematoporphyrin PDT drug, is active on photoirradiation at 630 nm, generating a $^1(\pi-\pi^*)$ state with subsequent formation of a $^3(\pi-\pi^*)$ triplet state that activates molecular oxygen to form reactive singlet oxygen ($^1O_2$) species in a type-II pathway. The skin toxicity and hepatotoxicity of the porphyrin-based drugs have generated interest in developing metal-based PDT drugs as alternatives.[21] While cisplatin and related compounds have found clinical applications as non-PDT metal-based chemotherapeutic drugs, dirhodium(II,II) complexes of polypyridyl ligands are reported to be potent PDT agents displaying photocytotoxicity in visible light.[22−26] A platinum(IV) complex having two photolabile azide ligands has recently been shown to be an effective cytotoxic agent on photoactivation, generating cisplatin at the cancer cells.[27] Ruthenium complexes are also known to show efficient photocytotoxicity.[28−30]

The present work stems from our interest in developing the chemistry of copper(II) complexes of α-amino acids as photocleavers of DNA in visible light, considering the biocompatibility of both the metal and the amino acids. Our earlier reports have shown that ternary copper(II) complexes of photoactive amino acids like L-lysine and L-methionine having DNA-binding phenanthroline bases are efficient photocleavers of DNA in red light.[31−34] We have observed that L-lysine with a cationic terminal amine group is a more efficient DNA photocleaver than L-methionine. This has prompted us to investigate the DNA photocleavage activity of ternary copper(II) complexes of L-arginine, as this α-amino acid with a cationic guanidinium terminal group could act as an efficient photosensitizer and, in addition, model the DNA-binding properties of sequence-specific DNA minor groove-binding molecules like netropsin (ntp). Additionally, L-arginine with its guanidinium group has the ability to form hydrogen bonds, as is known from the sequence selective binding of various DNA-binding proteins having L-arg as the major amino acid residues.[35] Netropsin is an antiviral antibiotic used extensively for biomedical applications for selective binding to the AT-rich sequences of DNA.[36−38] It has a crescent-shaped molecular structure that makes it an efficient binder to DNA. The biological activity of netropsin results due to its interfering with the proteins that regulate replication and transcription processes.[39] Since netropsin lacks any visible band in the PDT window of 630−800 nm, in the unmodified form or its amino acid/peptide analogues it could only cleave DNA in UV light.[36] Netropsin derivatives bound to transition metal ions are previously known to show sequence-selective chemical nuclease and hydrolase activities.[36,39−41] Literature reports have shown that amino acids and peptides tethered with photoactive organic molecules generally cleave DNA on irradiation with only UV light.[42−44] To circumvent the predicament of observing any photocleavage activity in the PDT window, we have chosen the crescent-shaped copper(II) bis-arginate complex (**1**) as a structural mimic of netropsin having end group similarities (Scheme 1). In addition, ternary copper(II) complexes [Cu(L-arg)(B)Cl]Cl (**2**−**5**), where B is a heterocyclic base, namely, 2,2′-bipyridine (bpy, **2**), 1,10-phenanthroline (phen, **3**), dipyrido[3,2-d:2′,3′-f]quinoxaline (dpq, **4**), and dipyrido[3,2-a:2′,3′-c]phenazine (dppz, **5**), and L-arg = L-arginine, are prepared to explore the effect of the presence of DNA binding phenanthroline bases on the photoinduced DNA

(11) Bonnett, R. *Chemical Aspects of Photodynamic Therapy*; Gordon and Breach: London, U.K., 2000.
(12) Detty, M. R.; Gibson, S. L.; Wagner, S. J. *J. Med. Chem.* **2004**, *47*, 3897.
(13) Szacilowski, K.; Macyk, W.; Drzewiecka-Matuszek, A.; Brindell, M.; Stochel, G. *Chem. Rev.* **2005**, *105*, 2647.
(14) Ali, H.; Van Lier, J. E. *Chem. Rev.* **1999**, *99*, 2379.
(15) De Rosa, M. C.; Crutchley, R. J. *Coord. Chem. Rev.* **2002**, *233/234*, 351.
(16) Henderson, B. W.; Busch, T. M.; Vaughan, L. A.; Frawley, N. P.; Babich, D.; Sosa, T. A.; Zollo, J. D.; Dee, A. S.; Cooper, M. T.; Bellnier, D. A.; Greco, W. R.; Oseroff, A. R. *Cancer Res.* **2000**, *60*, 525.
(17) Sessler, J. L.; Hemmi, G.; Mody, T. D.; Murai, T.; Burrell, A.; Young, S. W. *Acc. Chem. Res.* **1994**, *27*, 43.
(18) Mathai, S.; Smith, T. A.; Ghiggino, K. P. *Photochem. Photobiol. Sci.* **2007**, *6*, 995.
(19) Kar, M.; Basak, A. *Chem. Rev.* **2007**, *107*, 2861.
(20) Verma, S.; Watt, G. M.; Mai, Z.; Hasan, T. *Photochem. Photobiol.* **2007**, *83*, 1.
(21) Moriwaki, S. I.; Misawa, J.; Yoshinari, Y.; Yamada, I.; Takigawa, M.; Tokura, Y. *Photodermatol. Photoimmunol. Photomed.* **2001**, *17*, 241. Ochsner, M. J. *Photochem. Photobiol. B* **1996**, *32*, 3.
(22) Lippard, S. J. *Biochemistry* **2003**, *42*, 2664. Jamieson, E. R.; Lippard, S. J. *Chem. Rev.* **1999**, *99*, 2467.
(23) Dhar, S.; Liu, Z.; Thomale, J.; Dai, H.; Lippard, S. J. *J. Am. Chem. Soc.* **2008**, *130*, 11467.
(24) Angeles-Boza, A. M.; Chifotides, H. T.; Aguirre, J. D.; Chouai, A.; Fu, P. K.-L.; Dunbar, K. R.; Turro, C. *J. Med. Chem.* **2006**, *49*, 6841.
(25) Fernández, M.-J.; Wilson, B.; Palacios, M.; Rodrigo, M.-M.; Grant, K. B.; Lorente, A. *Bioconjugate Chem.* **2007**, *18*, 121.
(26) Jain, A.; Slebodnick, C.; Winkel, B. S. J.; Brewer, K. J. *J. Inorg. Biochem.* **2008**, *102*, 1854. Holder, A. A.; Swavey, S.; Brewer, K. J. *Inorg. Chem.* **2004**, *43*, 303.
(27) Mackay, F. S.; Woods, J. A.; Heringová, P.; Kašpárková, J.; Pizarro, A. M.; Moggach, S. A.; Parsons, S.; Brabec, V.; Sadler, P. J. *Proc. Natl. Acad. Sci. U. S. A.* **2007**, *104*, 20743.
(28) Rose, M. J.; Fry, N. L.; Marlow, R.; Hinck, L.; Mascharak, P. K. *J. Am. Chem. Soc.* **2008**, *130*, 8834.
(29) Brindell, M.; Kuliś, E.; Elmroth, S. K. C.; Urbańska, K.; Stochel, G. *J. Med. Chem.* **2005**, *48*, 7298.
(30) Karidi, K.; Garoufis, A.; Tsipis, A.; Hadjiliadis, N.; den Hulk, H.; Reedijk, J. *Dalton Trans.* **2005**, 1176.
(31) Patra, A. K.; Dhar, S.; Nethaji, M; Chakravarty, A. R. *Chem. Commun.* **2003**, 1562.
(32) Patra, A. K.; Nethaji, M.; Chakravarty, A. R. *Dalton Trans.* **2005**, 2798.
(33) Patra, A. K.; Dhar, S.; Nethaji, M.; Chakravarty, A. R. *Dalton Trans.* **2005**, 896.
(34) Patra, A. K.; Nethaji, M.; Chakravarty, A. R. *J. Inorg. Biochem.* **2007**, *101*, 233.
(35) Nelson, H. C. M. *Curr. Opin. Genet. Dev.* **1995**, *5*, 180.
(36) Bailly, C.; Chaires, J. B. *Bioconjugate Chem.* **1998**, *9*, 513.
(37) Neidle, S. *Nat. Prod. Rep.* **2001**, *18*, 291.
(38) Zimmer, Z.; Wähnert, U. *Prog. Biophys. Mol. Biol.* **1986**, *47*, 31.
(39) Chiang, S.-Y.; Welch, J.; Rauscher, F. J.; Beerman, T. A. *Biochemistry* **1994**, *33*, 7033.
(40) Welch, J.; Schultz, P. G.; Dervan, P. B. *Proc. Natl. Acad. Sci. U. S. A.* **1983**, *80*, 6834.
(41) Welch, J. J.; Rauscher, F. J.; Beerman, T. A. *J. Biol. Chem.* **1994**, *269*, 31051.
(42) Mahon, K. P., Jr.; Ortiz-Meoz, E. G.; Prestwich, R. F.; Kelly, S. O. *Chem. Commun.* **2003**, 1956.
(43) Wittenhagen, L. M.; Carreon, J. R.; Prestwich, E. G.; Kelley, S. O. *Angew. Chem., Int. Ed.* **2005**, *44*, 2542.
(44) Breiner, B.; Schlatterer, J. C.; Kovalenko, S. V.; Greenbaum, N. L.; Alabugin, I. V. *Angew. Chem., Int. Ed.* **2006**, *45*, 3666.

Scheme 1. The Crescent Shaped Structures of Netropsin (ntp) and $[Cu(L\text{-}arg)_2]^{2+a}$

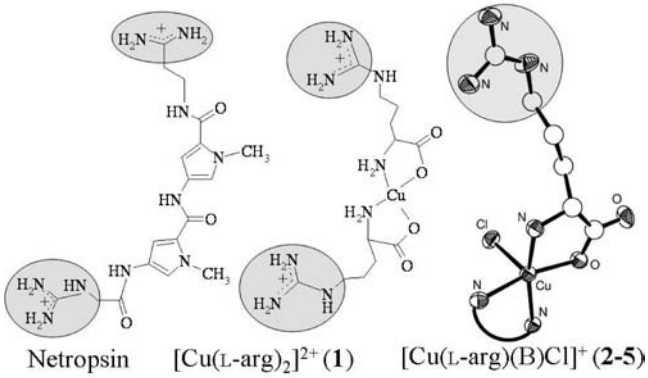

[a] The bent structure of the ternary copper(II) complexes is also shown.

Scheme 2. Binary and Ternary Copper(II) Complexes and the Heterocyclic Bases Used

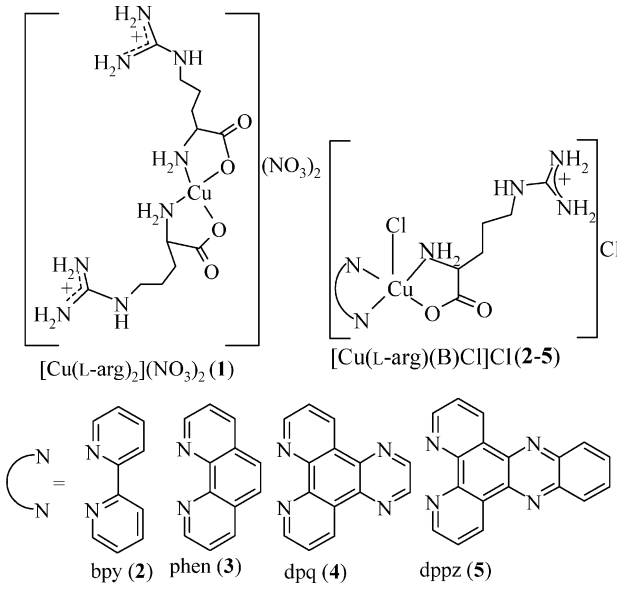

cleavage activity (Scheme 2). We have studied in detail the role of positively charged guanidinium group of L-arginine and the extended planar aromatic rings of the phenanthroline bases on sequence-specific DNA binding and photoinduced DNA cleavage activity. A preliminary report of this work using the complexes **1** and **3** has been made.[45] The significant results of this full report include observation of double-strand breaks (dsb) of DNA in red light for the dpq (**4**) and dppz (**5**) complexes. Complex **5** exemplifies a major groove-binding α-amino acid copper(II) complex showing dsb of DNA within the PDT window.

Experimental Section

Materials and Methods. All reagents and chemicals were purchased from commercial sources (Aldrich, USA; SD Fine Chemicals, India) and used as received without further purification. The supercoiled (SC) pUC19 DNA (CsCl purified) was procured from Bangalore Genie (India). Calf thymus (CT) DNA, agarose (molecular biology grade), distamycin, methyl green, catalase, superoxide dismutase (SOD) isolated from human erythrocytes (EC 232-943-0), netropsin dihydrochloride (ntp·2HCl), poly(dA)·poly(dT), poly(dG)·poly(dC), and ethidium bromide (EB) were purchased from Sigma (USA). Tris(hydroxymethyl)aminomethane−HCl (Tris-HCl) buffer was prepared using deionized and sonicated triple-distilled water. Solvents used for electrochemical and spectral measurements were purified according to reported procedures.[46] Dipyrido[3,2-*d*:2′,3′-*f*]quinoxaline and dipyrido[3,2-*a*:2′,3′-*c*]phenazine were prepared following reported methods.[47,48] $[Cu(L\text{-}arg)_2](NO_3)_2$ (**1**) was prepared using a literature method.[49]

The elemental analysis was done using a Thermo Finnigan FLASH EA 1112 CHNS analyzer. The infrared, electronic, and fluorescence spectra were recorded using Perkin-Elmer Lambda 35, Perkin-Elmer spectrum one 55, and Perkin-Elmer LS 50B spectrometers, respectively, at 25 °C. Room-temperature magnetic susceptibility data were obtained from a George Associates Inc. (Berkeley, CA) make Lewis-coil force magnetometer using Hg-$[Co(NCS)_4]$ as a standard. Experimental susceptibility data were corrected for diamagnetic contributions.[50] Molar conductivity measurements were made using a Control Dynamics (India) conductivity meter. Cyclic voltammetric measurements were made at 25 °C on an EG&G PAR model 253 VersaStat potentiostat/galvanostat with electrochemical analysis software 270 using a three-electrode setup consisting of a glassy carbon working, platinum wire auxiliary, and a saturated calomel reference electrode (SCE) in DMF-Tris buffer (1:1 v/v). Tetrabutylammonium perchlorate (TBAP; 0.1 M) was used as a supporting electrolyte for the electrochemical measurements.

Preparation of [Cu(L-arg)(B)Cl]Cl (B = bpy, 2; phen, 3; dpq, 4; dppz, 5). The complexes were prepared according to a general synthetic method in which an aqueous solution of $CuCl_2 \cdot 2H_2O$ (0.17 g, 1.0 mmol) was initially reacted with an aqueous solution of L-arginine (0.23 g, 1.1 mmol) treated with NaOH (0.040 g, 1.0 mmol), and this was followed by the slow addition of the corresponding heterocyclic base [0.15 g, bpy, **2**; 0.18 g, phen, **3**; 0.22 g, dpq, **4**; 0.28 g, dppz, **5** (0.9 mmol)] taken in 20 mL of methanol while stirring at 25 °C for 2 h and filtered. Slow evaporation of the filtrate yielded a crystalline solid of the product. The solid was isolated, washed with cold aqueous methanol (1:1 v/v), and dried over P_4O_{10} [yield: ∼75%]. Anal. calcd for $C_{16}H_{22}Cl_2CuN_6O_2$ (**2**): C, 41.34; H, 4.77; N, 18.08. Found: C, 41.27; H, 4.65; N, 17.86. FT-IR (KBr phase, cm^{-1}): 3373br, 3194br, 3027m, 1684s, 1660vs, 1601s, 1497m, 1477m, 1445s, 1378m, 1343m, 1323w, 1163m, 1122w, 1031w, 769s, 730m, 572m, 414m (br, broad; vs, very strong; s, strong; m, medium; w, weak). UV−visible in aqueous DMF (1:1 v/v) [λ_{max}/nm (ε/M^{-1} cm^{-1})]: 300 (8200), 598 (45). Λ_M (S m^2 M^{-1}) in water at 25 °C: 140. μ_{eff} (298 K) = 1.77 μ_B at 25 °C. Anal. calcd for $C_{18}H_{22}Cl_2CuN_6O_2$ (**3**): C, 44.22; H, 4.54; N, 17.19. Found: C, 44.12; H, 4.45; N, 16.94. IR (KBr phase, cm^{-1}): 3373br, 3194br, 3027br, 1684s, 1660vs, 1601s, 1497m, 1477m, 1445s, 1378s, 1343m, 1323w, 1156m, 1122w, 1031w, 769s, 730m, 572m, 414m. UV−visible in aqueous DMF (1:1 v/v) [λ_{max}/nm (ε/M^{-1} cm^{-1})]: 204 (33 600), 223 (29 300), 273 (29 700), 294 (9000), 600 (70). Λ_M (S m^2 M^{-1}) in water at 25 °C: 162. μ_{eff} = 1.76 μ_B at 25 °C. Anal. calcd for $C_{20}H_{22}Cl_2CuN_8O_2$ (**4**): C, 44.41; H, 4.10; N, 20.72. Found: C, 44.54; H, 4.02; N, 20.57. IR (KBr phase, cm^{-1}): 3344br, 3162br,

(45) Patra, A. K.; Bhowmick, T.; Ramakumar, S.; Chakravarty, A. R. *Inorg. Chem.* **2007**, *46*, 9030.

(46) Perrin D. D.; Armarego, W. L. F.; Perrin, D. R. *Purification of Laboratory Chemicals*; Pergamon Press: Oxford, U. K., 1980.

(47) Dickeson, J. E.; Summers, L. A. *Aust. J. Chem.* **1970**, *23*, 1023.

(48) Collins, J. G.; Sleeman, A. D.; Aldrich-Wright, J. R.; Greguric, I.; Hambley, T. W. *Inorg. Chem.* **1998**, *37*, 3133.

(49) Masuda, H.; Odani, A.; Yamazaki, T.; Yajima, T.; Yamauchi, O. *Inorg. Chem.* **1993**, *32*, 1111.

(50) Khan, O. *Molecular Magnetism*; VCH: Weinheim, Germany, 1993.

Table 1. Selected Crystallographic Data for [Cu(L-arg)(phen)Cl]Cl·2.5H_2O (**3**·2.5H_2O)

	3·2.5H_2O
formula	$C_{18}H_{27}Cl_2CuN_6O_{4.5}$
fw, g M^{-1}	533.90
cryst syst	triclinic
space group (no.)	*P*1 (1)
a, Å	10.359(6)
b, Å	12.437(7)
c, Å	18.888(11)
α, deg	94.599(9)
β, deg	104.701(9)
γ, deg	101.002(9)
V, Å^3	2289(2)
Z	4
T, K	293(2)
ρ_{calcd}, g cm^{-3}	1.549
λ, Å (Mo Kα)	0.71073
μ, mm^{-1}	1.227
data/restraints/parameter	17447/3/1136
GoF on F^2	1.025
R (F_0)[a] ($I > 2\sigma(I)$) [R all data]	0.0454 [0.0588]
wR (F_0)[b] ($I > 2\sigma(I)$) [wR all data]	0.1226 [0.1326]
largest diff. peak, hole (e. Å^{-3})	0.934, −0.532
$w = 1/[\sigma^2(F_o^2) + (AP)^2 + (BP)]$	A = 0.0789, B = 0.0

[a] $R = \sum||F_o| - |F_c||/\sum|F_o|$. [b] $wR = \{\sum[w(F_o^2 - F_c^2)^2]/\sum[w(F_o)^2]\}^{1/2}$, $w = [\sigma^2(F_o)^2 + (AP)^2 + BP]^{-1}$, where $P = (F_o^2 + 2F_c^2)/3$.

1651s, 1633vs, 1580s, 1487m, 1470m, 1449m, 1405s, 1386s, 1310w, 1175m, 1116m, 1083m, 890w, 823m, 732s, 649m, 606m, 557w. UV−visible in aqueous DMF (1:1 v/v) [λ_{max}/nm (ε/M^{-1} cm^{-1})]: 258 (23 600), 340 (2760), 632 (135). Λ_M (S m^2 M^{-1}) in water at 25 °C: 132. μ_{eff} = 1.75 μ_B. Anal. calcd for $C_{24}H_{24}Cl_2CuN_8O_2$ (**5**): C, 48.78; H, 4.09; N, 18.96. Found: C, 48.64; H, 3.96; N, 18.78. IR (KBr phase, cm^{-1}): 3698br, 3046br, 2962br, 1621s, 1574s, 1495s, 1487s, 1465w, 1438m, 1358m, 1338w, 1261w, 1074s, 1047w, 816s, 766s, 731s, 566w, 579w, 420m. UV−visible in aqueous DMF (1:1 v/v) [λ_{max}/nm (ε/M^{-1} cm^{-1})]: 271(48 400), 361 (11 500), 378 (11 400), 683 (120). Λ_M (S m^2 M^{-1}) in water at 25 °C: 128. μ_{eff} = 1.79 μ_B at 25 °C.

Solubility and Stability. The complexes showed good solubility in DMF, DMSO, and water; showed less solubility in methanol and ethanol; and were insoluble in hydrocarbons. They showed stability in the solid as well as in the solution phase.

X-Ray Crystallographic Procedures. Single crystals of **3** were obtained on slow evaporation of the reaction mixture of the complex. The crystal structure of [Cu(L-arg)(phen)Cl]Cl·2.5H_2O (**3**·2.5H_2O) was obtained using single-crystal X-ray diffraction techniques. Crystal mounting was done on a glass fiber with epoxy cement. All geometric and intensity data were collected at room temperature using an automated Bruker SMART APEX CCD diffractometer equipped with a fine-focus 1.75-kW sealed-tube Mo Kα X-ray source (λ = 0.71073 Å) with increasing ω (width of 0.3° per frame) at a scan speed of 12 s/frame. The intensity data were corrected for Lorentz-polarization effects and for absorption.[51] The structure was solved and refined with the SHELX system of programs.[52] The hydrogen atoms were fixed in their calculated positions and refined using a riding model. All non-hydrogen atoms were refined anisotropically. Selected crystal data for the complex are summarized in Table 1. A perspective view of the complex was obtained using ORTEP.[53]

DNA Binding Experiments. The binding experiments were carried out in Tris-HCl buffer (5 mM, pH 7.2) using aqueous solutions of the complexes. CT DNA (ca. 300 μM NP) in the buffer medium gave a ratio of the UV absorbances at 260 and 280 nm of ca. 1.9:1, suggesting that the CT DNA was apparently free from protein.[54] The concentrations of the homopolymers and CT DNA were determined using UV−visible spectroscopy using the following λ_{max} values, nm (ε, M^{-1} cm^{-1}), in the buffer: poly(dA)·poly(dT), 260 (6000); poly(dG)·poly(dC), 253 (7400); and CT-DNA, 260 (6600).[55] Absorption titration experiments were performed upon varying the concentration of CT DNA, keeping the metal complex concentration constant. Due correction was made for the absorbance of DNA itself. All of the UV spectra were recorded after equilibration of the solution for 5 min. The intrinsic equilibrium DNA binding constants (K_b) along with the binding site size (s) of the complexes of CT DNA were determined by monitoring the change of the absorption intensity of the ligand-centered charge-transfer spectral band with increasing concentration of the CT DNA with a regression analysis using eq 1:

$$(\varepsilon_a - \varepsilon_f)/(\varepsilon_b - \varepsilon_f) = [b - (b^2 - 2K_b^2C_t[\mathrm{DNA}]/s)^{1/2}]/2K_bC_t \quad (1)$$

$$b = 1 + K_bC_t + K_b[\mathrm{DNA}]/2s$$

where ε_a is the extinction coefficient of the charge-transfer band at a given DNA concentration, ε_f is the extinction coefficient of the complex free in solution, ε_b is the extinction coefficient of the complex when fully bound to DNA, K_b is the equilibrium binding constant, C_t is the total metal complex concentration, [DNA] is the DNA concentration in nucleotides, and s is the binding site size in base pairs.[56,57] The theoretical fit was based on the assumption of noncooperative metallointercalator binding of the complexes to DNA.

The apparent binding constant (K_{app}) values of complexes **1**−**5** were obtained by fluorescence spectral technique using an EB-bound DNA solution in Tris-HCl/NaCl buffer (pH, 7.2). The fluorescence intensities of EB at 600 nm (546 nm excitation) were recorded with an increasing quantity of the ternary complex concentration. EB was nonemissive in the Tris-buffer medium due to fluorescence quenching of the free EB by the solvent molecules.[58,59] In the presence of DNA, EB showed enhanced emission intensity due to its binding to DNA. A competitive binding of the copper complexes to DNA could result in either the displacement of bound EB or emission quenching resulting in a decrease of its emission intensity. The K_{app} values were obtained from the equation $K_{app} \times [\mathrm{complex}]_{50} = K_{EB} \times [\mathrm{EB}]$, where K_{app} is the apparent binding constant of the complex studied, $[\mathrm{complex}]_{50}$ is the concentration of the complex at 50% quenching of DNA-bound EB emission intensity, K_{EB} is the binding constant of EB ($K_{EB} = 1.0 \times 10^7$ M^{-1}), and [EB] is the concentration of EB (1.3 μM).[60]

DNA-melting experiments were carried out by monitoring the absorbance of DNA (150 μM NP) at 260 nm at various temperatures in the absence and presence of the complexes in a 2:1 ratio of the DNA and complex, with a ramp rate of 0.5 °C/min in a phosphate buffer medium (pH 6.85) using a Peltier system attached to the

(51) Walker, N.; Stuart, D. *Acta Crystallogr.* **1983**, *A39*, 158.
(52) Sheldrick, G. M. *SHELX-97*; University of Göttingen, Göttingen, Germany, 1997.
(53) Johnson, C. K. *ORTEP-III, Report ORNL - 5138*; Oak Ridge National Laboratory: Oak Ridge, TN, 1976.
(54) Marmur, J. *J. Mol. Biol.* **1961**, *3*, 208.
(55) Foxon, S. P.; Metcalfe, C.; Adams, H.; Webb, M.; Thomas, J. A. *Inorg. Chem.* **2007**, *46*, 409.
(56) McGhee, J. D.; von Hippel, P. H. *J. Mol. Biol.* **1974**, *86*, 469.
(57) Carter, M. T.; Rodriguez, M.; Bard, A. J. *J. Am. Chem. Soc.* **1989**, *111*, 8901.
(58) Waring, M. *J. Mol. Biol.* **1965**, *13*, 269.
(59) LePecq, J.-B.; Paoletti, C. *J. Mol. Biol.* **1967**, *27*, 87.
(60) Lee, M.; Rhodes, A. L.; Wyatt, M. D.; Forrow, S.; Hartley, J. A. *Biochemistry* **1993**, *32*, 4237.

UV−visible spectrophotometer. Viscometric titrations were done using a Schott Gerate AVS 310 Automated Viscometer. The viscometer was thermostatted at 37 °C in a constant-temperature bath. The concentration of DNA was 160 μM in NP, and the flow times were measured with an automated timer. Each sample was measured three times, and an average flow time was calculated. The relative solution viscosity (η/η_0) and contour length (L/L_0) are related by $L/L_0 = (\eta/\eta_0)^{1/3}$, where L_0 and η_0 denote the apparent molecular length and solution viscosity, respectively, in the absence of the metal complex.[61] The data were plotted as $(\eta/\eta_0)^{1/3}$ versus [complex]/[DNA], where η is the viscosity of DNA in the presence of the complex and η_0 is that of DNA alone. Viscosity values were calculated from the observed flow time of DNA-containing solutions (t) corrected for that of the buffer alone (t_0), $\eta = (t - t_0)$.

Molecular Docking Calculations. Molecular docking calculations were done using the DS Modeling 1.2-SBD Docking Module by Accelrys Software.[62] The CHARMm force-field was used for the metal complex in the input of the calculations. Due to the higher hybridization state of the copper atom in the complex, due correction of the partial charge distribution for all atoms in the ligand was made following the output from Gaussian 03.[63] Energy-minimized structures of complexes **4** and **5** were generated from the coordinates of the crystal structure of complex **3**. Model building and optimization were performed using the DS Modeling 1.1 SBD model-building and energy-minimization modules of the Accelrys Software Package. After making the necessary changes, the model was subjected to energy minimization via conjugate gradient steps. The crystal structure of the B-DNA dodecamer d(CGCGAATTCGCG)$_2$ (NDB code GDLB05) was downloaded from the protein data bank (PDB). Polymeric $(dAdT)_6$ was constructed with model building followed by energy minimization. In the docking analysis, the binding site was assigned across the all of the minor and major grooves of the DNA molecule. The docking was performed to find the most stable and favorable orientation.

The docking options consisted of the following steps: (i) Monte Carlo options to perform a flexible fit, (ii) thresholds for diversity of the saved pose (defined to 2 Å to scan through different conformations), (iii) pose optimization done in two steps, (a) steepest descent minimization and (b) BFGS rigid body minimization, (iv) ligand internal energy optimization and filtering poses with short contacts (VDW and electrostatic energy calculated), and (v) pose filtering and processing. Dock scores for conformations above 2 kcal M^{-1} energy were accepted. Clustering of the poses using the leader algorithm was done. Scoring for the docked poses was determined primarily using a Ludi score that included five major contributions: (a) contributions from ideal hydrogen bonds, (b) contributions from perturbed ionic interaction, (c) contributions from lipophilic interaction, (d) a contribution due to the freezing of internal degrees of freedom, and (e) contributions due to a loss of translational and rotational entropy of the ligand. The optimum docking state with the highest energy stabilization was obtained in a two-stage docking, where following the previously mentioned steps the initial docking was performed. After the thorough analysis of different docked poses and the corresponding conformations of the metal complexes, the second stage of docking was performed in an energy-profile-guided manner depending upon the best binding trends using the top-scored conformations of the ligand obtained as outputs from the first-stage docking.

DNA Cleavage Experiments. The cleavage of supercoiled pUC19 DNA (30 μM, 0.2 μg, 2686 base pairs) by the copper(II) complexes was studied using agarose gel electrophoresis in a 50 mM Tris-HCl buffer (pH 7.2) containing 50 mM NaCl. To study the chemical nuclease activity of the complexes, SC DNA was treated with the complex and 3-mercaptopropionic acid (MPA, 0.5 mM) as a reducing agent in the dark. Photoinduced DNA cleavage studies were carried out under illuminated conditions using a UV-A source of 365 nm (Bangalore Genie make, 6 W power, sample area of illumination of 45 mm^2) and 647.1 nm using a continuous-wave (CW) Ar−Kr laser (100 mW laser power; laser beam diameter, 1.8 mm; beam divergence, 0.70 mrad; Spectra Physics Water-Cooled Mixed-Gas Ion Laser Stabilite 2018-RM). The power of the laser beam was measured using a Spectra Physics CW Laser Power Meter (model 407A) at the sample position. Eppendorf and glass vials were used for respective UV-A and visible-light experiments in a dark room at 25 °C using SC DNA (1 μL, 30 μM) in a 50 mM Tris-HCl buffer (pH 7.2) containing 50 mM NaCl and the complex (2 μL in H_2O) with varied concentrations. The concentration of the complexes or the additives reported in this work corresponded to that in the 20 μL final volume using Tris-HCl buffer. The solution path length used for illumination in the sample vial was ∼5 cm. After the photoexposure, the sample was incubated for 1 h at 37 °C, followed by its addition to the loading buffer containing 25% bromophenol blue, 0.25% xylene cyanol, and 30% glycerol (3 μL), and the solution was finally loaded on 1.2% agarose gel containing 1.0 μg mL^{-1} ethidium bromide. The electrophoresis was carried out in a dark room for 2 h at 45 V in a Tris-acetate-EDTA buffer. The bands were visualized by UV light and photographed. The extent of cleavage of SC DNA was determined by measuring the intensities of the bands using a UVITECH Gel Documentation System. Due corrections were made for the low level of the nicked circular (NC) form present in the original SC DNA sample and for the low affinity of EB binding to SC compared to that to NC and linear forms of DNA.[64] The error in measuring %NC and linear forms from the gel electrophoresis diagrams ranged between 3 and 5%. The mechanistic studies were carried out on adding various additives (distamycin, 10 μM; methyl green, 10 μM; DMSO, 4 μL; sodium azide, 100 μM; mannitol, 100 μM; KI, 100 μM; catalase, 4 units; SOD, 4 units) prior to the addition of the complex. For the D_2O experiment, this solvent was used for dilution of the sample volume to 20 μL.

Results and Discussion

Synthesis and General Aspects. Ternary copper(II) complexes of the formulation [Cu(L-arg)(B)Cl]Cl (**2**−**5**) have been synthesized in high yield by reacting the in situ generated sodium salt of L-arginine with $CuCl_2 \cdot 2H_2O$ and

(61) Cohen, G.; Eisenberg, H. *Biopolymers* **1969**, *8*, 45.
(62) Structure-Based Drug Design with Discovery Studio: *Accelrys*, version 0406; Accelrys Software Inc.: San Diego, CA, 2003.
(63) Frisch, M. J.; Trucks, G. W.; Schlegel, H. B.; Scuseria, G. E.; Robb, M. A.; Cheeseman, J. R.; Montgomery, J. A., Jr.; Vreven, T.; Kudin, K. N.; Burant, J. C.; Millam, J. M.; Iyengar, S. S.; Tomasi, J.; Barone, V.; Mennucci, B.; Cossi, M.; Scalmani, G.; Rega, N.; Petersson, G. A.; Nakatsuji, H.; Hada, M.; Ehara, M.; Toyota, K.; Fukuda, R.; Hasegawa, J.; Ishida, M.; Nakajima, T.; Honda, Y.; Kitao, O.; Nakai, H.; Klene, M.; Li, X.; Knox, J. E.; Hratchian, H. P.; Cross, J. B.; Adamo, C.; Jaramillo, J.; Gomperts, R.; Stratmann, R. E.; Yazyev, O.; Austin, A. J.; Cammi, R.; Pomelli, C.; Ochterski, J. W.; Ayala, P. Y.; Morokuma, K.; Voth, G. A.; Salvador, P.; Dannenberg, J. J.; Zakrzewski, V. G.; Dapprich, S.; Daniels, A. D.; Strain, M. C.; Farkas, O.; Malick, D. K.; Rabuck, A. D.; Raghavachari, K.; Foresman, J. B.; Ortiz, J. V.; Cui, Q.; Baboul, A. G.; Clifford, S.; Cioslowski, J.; Stefanov, B. B.; Liu, G.; Liashenko, A.; Piskorz, P.; Komaromi, I.; Martin, R. L.; Fox, D. J.; Keith, T.; Al-Laham, M. A.; Peng, C. Y.; Nanayakkara, A.; Challacombe, M.; Gill, P. M. W.; Johnson, B.; Chen, W.; Wong, M. W.; Gonzalez, C.; Pople, J. A. *Gaussian 03*, revision C.02; Gaussian Inc.: Wallingford, CT, 2004.
(64) Bernadou, J.; Pratviel, G.; Bennis, F.; Girardet, M.; Meunier, B. *Biochemistry* **1989**, *28*, 7268.

Table 2. Selected Physicochemical Data for the Complexes **1**−**5**

complex	d−d band: λ_{max}/nm (ε/M^{-1} cm^{-1})[a]	$E_{1/2}$/V (ΔE_p/mV)[b]	μ_{eff}[c]/μ_B
1	630 (80)	−0.38 (330)	1.78
2	598 (45)	0.04 (120)	1.77
3	600 (70)	0.01 (150)	1.76
4	632 (135)	0.15 (100)	1.75
5	683 (120)	−0.02 (365)	1.79

[a] In aqueous DMF (1:1 v/v). [b] Cu(II)−Cu(I) redox couple in DMF−Tris buffer (1:1 v/v) with 0.1 M TBAP as the supporting electrolyte. $E_{1/2} = 0.5(E_{pa} + E_{pc})$, $\Delta E_p = E_{pa} - E_{pc}$, where E_{pa} and E_{pc} are the anodic and cathodic peak potentials, respectively. Potentials are versus SCE. Scan rate = 50 mV s^{-1}. [c] Magnetic moment (μ_{eff}) using solid-state samples at 298 K.

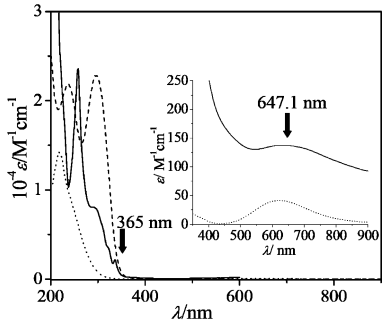

Figure 1. Electronic spectra of netropsin (----), **1** (····), and **4** (—) in aqueous DMF (1:1 v/v) with the inset showing the d−d band of the copper(II) complexes **1** and **4** and the wavelengths used for photoinduced DNA cleavage studies.

the heterocyclic base, where B is the N,N-donor bpy (**2**), phen (**3**), dpq (**4**), and dppz (**5**) (Scheme 2). We have also prepared a known binary complex, [Cu(L-arg)$_2$](NO$_3$)$_2$ (**1**), as a model for the AT-selective DNA binder netropsin.[49] Among the four heterocyclic bases used, dpq and dppz are photoactive in UV light.[65] The complexes are characterized from their analytical and physicochemical data (Table 2). The one-electron paramagnetic copper(II) complexes exhibit a broad d−d band in the range of 590−690 nm in aqueous DMF with a molar extinction coefficient value of 45−135 M^{-1} cm^{-1}. The dpq and dppz complexes show a moderately strong band near 350 nm possibly due to $n-\pi^*$ transition involving the quinoxaline or phenazine moieties of the ligands, and this band is not observed in the bpy and phen complexes (Figure 1).[66−68] All of the complexes are redox-active, displaying a quasireversible cyclic voltammetric response assignable to the Cu(II)/Cu(I) couple in the range of −0.1 to −0.3 V (vs SCE) in a DMF-Tris-HCl buffer (Figure S1, Supporting Information).

Crystal Structure. The phen complex **3** has been structurally characterized in a single-crystal X-ray diffraction study.[45] The complex crystallizes in the noncentrosymmetric *P*1 space group of the triclinic crystal system, having four independent molecules ($Z = 4$) in the crystallographic asymmetric unit that is the unit cell (Figure S2, Supporting Information). The crystal structure shows the monocationic nature of the complex having chelating bidentate L-arginine bonded through amine-N and carboxylate-O and the presence of a N,N donor, 1,10-phenanthroline, in a square-pyramidal (4 + 1) geometry, having a weak axially bound chloride ligand ($\tau_{av} = 0.08$).[69] The ORTEP view of the complex is shown in Figure 2. Selected bond distances and angles of four independent complex units belonging to the unit cell are given in Table S1 (Supporting Information). The average Cu−O (L-arg), Cu−N (L-arg), Cu−N (phen), and Cu−Cl distances are 1.941[5], 1.996[5], 2.017[5], and 2.556[2] Å, respectively. The alkyl chain containing the positively charged guanidinium group of L-arginine remains as a pendant moiety. The structure shows the presence of extensive intermolecular hydrogen-bonding interactions. The hydrogen atoms of NH$_2$ in the guanidinium group are bonded to the carboxyl oxygen atom (distance ∼2.9−3.0 Å) of another molecule and the lattice water molecules. Ionic contacts between the positively charged guanidinium group and lattice chloride and water molecules are also visible in the crystal lattice. Complex **3** partially models the molecular structure of netropsin that has a crescent-shaped structure with the amide groups on the concave side and the carbonyl and methyl groups on the convex side.[38] The reported molecular structure of [Cu(L-arg)$_2$](NO$_3$)$_2$ (**1**) has the copper(II) in a square-planar geometry with the L-arginine ligands in a cis configuration, giving a netropsin-shaped structure. The binary complex presents a better structural model for netropsin than the ternary complexes.[49]

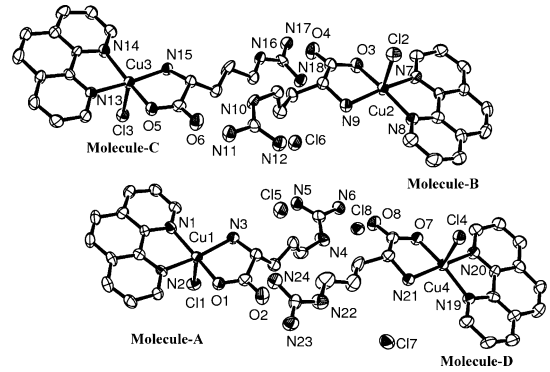

Figure 2. ORTEP views of four independent molecules (molecules A−D) in the asymmetric unit of [Cu(L-arg)(phen)Cl]Cl·2.5H$_2$O (**3**·2.5H$_2$O) showing the atom labeling scheme for only the metal and heteroatoms with 50% probability thermal ellipsoids. Selected average bond distances (Å) and angles (deg) are Cu−O (L-arg), 1.941[5]; Cu−N (L-arg), 1.996[5]; Cu−N (phen), 2.017[5]; Cu−Cl, 2.556[2]; ∠N−Cu−N (phen), 81.5[2]; ∠O−Cu−N (L-arg), 84.1[2].

DNA Binding Studies. The mode and propensity of binding of ntp and the complexes to the CT DNA, poly(dA)·poly(dT), and poly(dG)·poly(dC) have been studied using different spectral technique, DNA thermal denaturation, and viscosity measurements (Table 3).

Electronic Spectral Studies. An absorption titration method has been used to monitor the interaction of netropsin and complexes **1**−**5** with CT-DNA (Figure 3). An intercalative binding of a complex to DNA generally leads to

(65) Toshima, K.; Takano, R.; Ozawa, T.; Matsumura, S. *Chem. Commun.* **2002**, 212.
(66) Armitage, B. *Chem. Rev.* **1998**, *98*, 1171.
(67) Roy, M.; Pathak, B.; Patra, A. K.; Jemmis, E. D.; Nethaji, M.; Chakravarty, A. R. *Inorg. Chem.* **2007**, *46*, 11122.
(68) McGovern, D. A.; Selmi, A.; O'Brien, J. E.; Kelly, J. M.; Long, C. *Chem. Commun.* **2005**, 1402.
(69) Addison, A. W.; Rao, T. N.; Reedijk, J. V.; Verschoor, G. C. *J. Chem. Soc., Dalton Trans.* **1984**, 1349.

Table 3. DNA Binding Parameters for Netropsin (ntp), $[Cu(L\text{-arg})_2](NO_3)_2$ (**1**), and [Cu(L-arg)(B)Cl]Cl (B = bpy, **2**; phen, **3**; dpq, **4**; dppz, **5**)

	poly(dA)·poly(dT)[a]			CT-DNA			poly(dG)·poly(dC)[a]	
	K_b[b]/M^{-1} (*s*)	K_{app}[c]/M^{-1}	ΔT_m[d]/°C	K_b/M^{-1} (*s*)[b]	K_{app}[c]/M^{-1}	ΔT_m/°C	K_b[b]/M^{-1} (*s*)	K_{app}[c]/M^{-1}
ntp	4.2×10^6 (0.34)	2.3×10^7	38	2.0×10^6 (0.3)	6.1×10^6	18	6.0×10^5 (0.12)	1.8×10^5
1	1.8×10^6 (0.24)	1.5×10^6	11	7.0×10^5 (0.12)	1.3×10^6	3	3.4×10^5 (0.28)	5.3×10^5
2				1.7×10^3 (0.4)	2.3×10^3	1.1		
3	2.6×10^6 (0.49)	1.1×10^6	8	1.2×10^5 (0.6)	9.3×10^5	2	9.3×10^4 (0.27)	4.9×10^5
4				4.2×10^5 (0.8)	1.2×10^6	3.1		
5				7.0×10^5 (0.9)	6.1×10^6	4.3		

[a] DNA binding studies using poly(dA)·poly(dT) and poly(dG)·poly(dC) were done for netropsin and the complexes **1** and **3**. Since the T_m of poly(dG)·poly(dC) was found to be 98 °C under the experimental conditions, it was not possible to study the effect of the binders on its thermal denaturation. [b] K_b, the equilibrium binding constant; *s*, the binding site size. [c] K_{app}, the apparent binding constant from ethidium bromide displacement assay. [d] DNA melting temperature (T_m) of poly(dA)·poly(dT) = 47 °C.

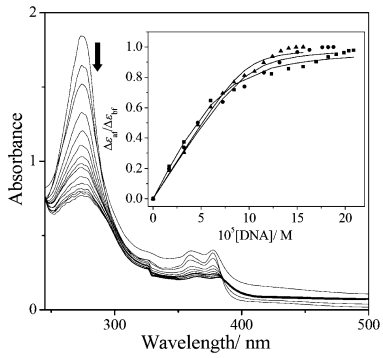

Figure 3. Absorption spectral traces of the dppz complex **5** (50 μM) on the addition of CT DNA in a Tris buffer medium (pH 7.2). The inset shows the plot of $\Delta\varepsilon_{af}/\Delta\varepsilon_{bf}$ vs [DNA], obtained from absorption spectral titration of the complexes **3** (■), **4** (●), and **5** (▲) with CT-DNA in Tris-buffer (pH 7.2), where $\Delta\varepsilon_{af} = (\varepsilon_a - \varepsilon_f)$ and $\Delta\varepsilon_{bf} = (\varepsilon_b - \varepsilon_f)$.

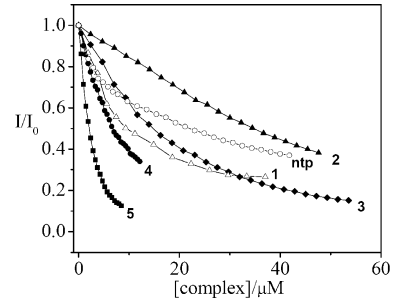

Figure 4. Effect of increasing the concentration of netropsin (ntp) (○), **1** (△), **2** (▲), **3** (♦), **4** (●), and **5** (■) on the emission intensity of ethidium bromide bound CT-DNA in a 5 mM Tris buffer−5 mM NaCl medium.

hypochromism along with a bathochromic shift of the electronic spectral bands resulting from strong stacking interaction between the aromatic chromophore of the ligand in the complex and the base pairs of the DNA.[70] On the basis of the extent of hypochromism among the present complexes, the observed DNA binding order is **5** (L-arg-Cu-dppz) ≥ **1** (bis-L-arg-Cu) > **4** (L-arg-Cu-dpq) > **3** (L-arg-Cu-phen) ≫ **2** (L-arg-Cu-bpy). It appears from the binding data of **2**−**5** that the DNA binding propensity of the complex increases with an increase in the extended planarity of the heterocyclic base. The extended planar aromatic ring(s) in dppz and dpq could insert between the base stack of DNA for intercalative binding. Interestingly, binary complex **1** shows better binding propensity than both **3** and **4**, having a planar phen and dpq as the DNA binder, respectively. The crescent-shaped molecular structure of **1** seems to make it an efficient DNA binder by providing strong noncovalent interactions and shape complementarity in the minor groove of ds-DNA. The intrinsic equilibrium DNA binding constants (K_b) along with the binding site size (*s*) of the complexes with DNA are determined by monitoring the change in the absorption intensity of the charge-transfer spectral bands of the compounds with increasing concentration of the DNA.[56,57] The fluorescence spectral method is used to study the relative binding of the complexes to DNA (Figure 4). The emission intensity of EB is used as a spectral probe, as it shows enhanced emission intensity when bound to the hydrophobic part of DNA. The binding of the complexes to DNA could result in the displacement of the bound EB and could cause a decrease in emission intensity due to quenching by the paramagnetic complexes. The DNA binding propensity of the present complexes is measured from the reduction of the emission intensity of EB at different complex concentrations. The K_{app} values obtained by this method have given an order which is similar to that obtained from the absorption titration measurements.

DNA Melting and Viscosity Studies. Binding of ntp and **1**−**5** to DNA has also been studied from the DNA melting experiment. A moderate positive shift in the DNA melting temperature (ΔT_m) is observed on the addition of the complexes to DNA (Figure 5a). The results primarily suggest the groove binding and electrostatic binding nature of the complexes to DNA in preference over an intercalative mode of binding to DNA that normally gives significantly high positive ΔT_m values.[71] To investigate further the binding nature of the complexes, viscosity measurements on the solutions of DNA incubated with the complexes have been carried out. Since the viscosity of a DNA solution is sensitive to the addition of a complex bound by intercalation, we have examined the change of the specific relative viscosity of DNA upon addition of the complexes. A classical DNA intercalating molecule like ethidium bromide causes lengthening of the DNA duplex upon the insertion of EB between the stacked bases, and this increases the relative viscosity. In contrast, a partial or nonclassical intercalation of the molecule could bend or kink DNA, resulting in a decrease in its effective length with a minor increase in its viscosity. The plots of relative viscosities with $1/R$ =[Cu]/[DNA] are shown in Figure 5b. The relative viscosity of DNA increases moderately with an increase in the concentration of the

(70) Barton, J. K.; Danishefsky, A. T.; Goldberg, J. M. *J. Am. Chem. Soc.* **1984**, *106*, 2172.

(71) Gunther, L. E.; Yong, A. S. *J. Am. Chem. Soc.* **1968**, *90*, 7323.

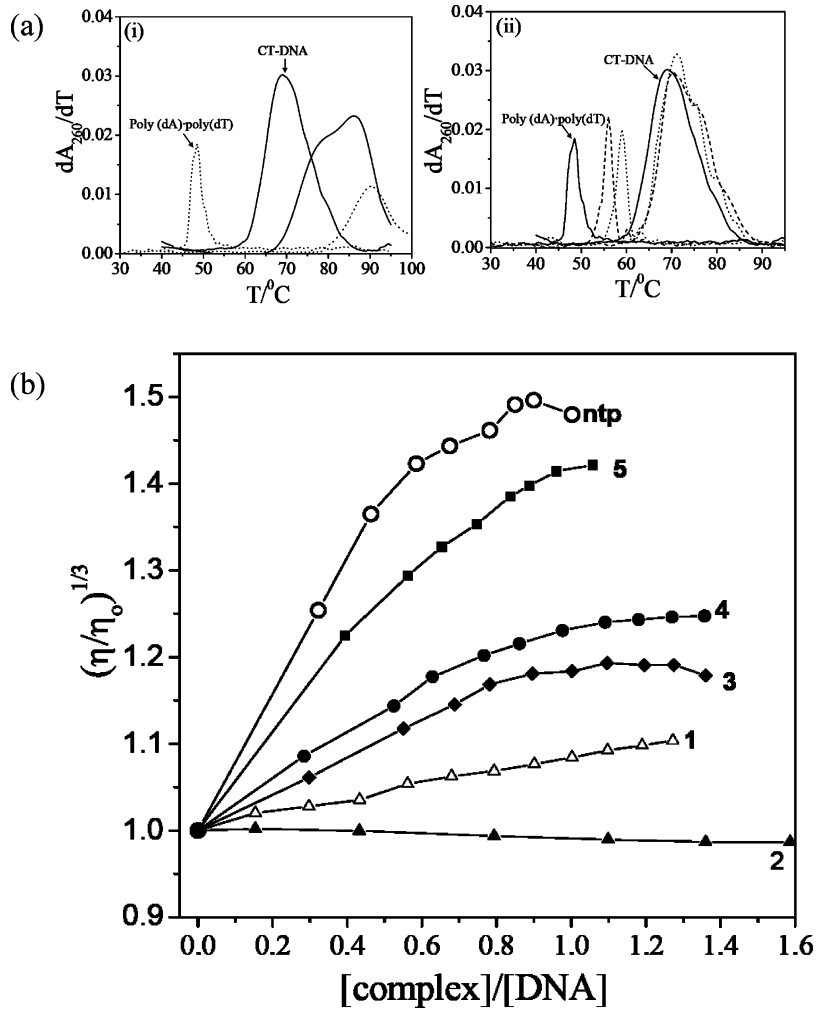

Figure 5. (a) Plots of $d(A_{260})/dT$ vs temperature for poly(dA)·poly(dT) (····); CT-DNA (—) with netropsin (i) and $[Cu(L\text{-arg})_2](NO_3)_2$ (**1**) (····) and [Cu(L-arg)(phen)Cl]Cl (**3**) (----) (ii) in a 5 mM Tris-buffer medium (pH 7.2) with a [DNA]/[ntp] = 20:1 and [DNA]/[complex] = 5:1. (b) Effect on relative specific viscosities of calf thymus DNA in the presence of netropsin (○), **2** (▲), **3** (♦), **4** (●), and **5** (■) in a 5 mM Tris buffer medium (pH 7.2) at 37.0 (±0.1) °C.

complexes. The η/η_0 values thus obtained follow the order ntp > **5** > **4** > **3** > **1** ≫ **2**. The results are consistent with the observed trend obtained for the ternary complexes from the spectral methods. The changes in relative viscosity for the dppz and dpq complexes are more than that for the phen analogue, suggesting greater DNA binding propensity of the dpq and dppz complexes. The bpy complex is a poor binder to DNA in the absence of any planar aromatic ring like the phenanthroline bases. Complex **1**, in the absence of any phenanthroline base, is more likely to have a DNA groove-binding propensity than any partial intercalative mode of binding as observed for the dpq and dppz complexes.

Sequence Selectivity. Selectivity is of paramount importance in designing efficient leads for drug discovery, as low selectivity leads to high toxicity and other side effects. To study the sequence selectivity of the complexes, we have carried out binding experiments using synthetic homo-oligomers, poly(dA)·poly(dT), poly(dG)·poly(dC), and mixed sequence CT DNA. Netropsin and the binary and ternary L-arginine copper(II) complexes show preferential binding to poly(dA)·poly(dT) in comparison to poly(dG)·poly(dC) or mixed-sequence CT DNA (Table 3, Figure 5a). The binding parameters (K_b, K_{app}, ΔT_m) of both the binary $[Cu(L\text{-arg})_2]^{2+}$ and representative ternary complex $[Cu(L\text{-arg})(phen)Cl]^+$ are higher with poly(dA)·poly(dT) than those with poly(dG)·poly(dC) or CT DNA, like netropsin. Such preferential binding of the L-arg complexes may be due to their crescent-shaped structure (shape resemblance) and the positively charged guanidinium end group similarity with netropsin (Scheme 1).

Molecular Docking Calculations. Molecular docking calculations have been carried out in order to gain insight into the binding interaction of L-arginine complexes **1** and **3** with a $d(CGCGAATTCGCG)_2$ dodecamer (NDB code: GDLB05; Table 4, Figure 6). The results show the binding of **1** to the phosphate backbone of the polynucleotide involving the terminal positively charged guanidinium end groups of L-arginine through H bonding (2.8−3.0 Å) and ionic contacts (Figure 6a; Figure S3, Supporting Information). The complex preferentially binds at the AT region of the dodecamer. The span of the AT-binding stretch is relatively short compared to netropsin due to a shorter overall length of the complex.[72] This finding is consistent with the binding parameters obtained from the spectroscopic methods.

Table 4. Hydrogen Bonding Interactions Involving the Energy-Minimized Docked Poses of d(CGCGAATTCGCG)$_2$ with **1** and **3** and poly(dA·dT)$_6$ for **4** and **5**[a]

acceptor group (Y−H)	donor group Z	distance (Å)
	[Cu(L-arg)$_2$](NO$_3$)$_2$ (**1**)	
N8−H37 (ligand)	O*4 A19 (DNA-Chain B)	2.65
N9−H39 (ligand)	O*4 C9 (DNA-Chain A)	2.84
N13−H53 (ligand)	O2 T6 (DNA-Chain A)	2.78
	[Cu(L-arg)(phen)Cl]Cl (**3**)	
N12−H13 (ligand)	O2 T6 (DNA-Chain A)	2.96
N12−H14 (ligand)	O2 T6 (DNA-Chain A)	2.79
N12−H13 (ligand)	N3 A20 (DNA-Chain B)	2.81
N9−H10 (ligand)	N3 A20 (DNA-Chain B)	3.04
N5−H7 (ligand)	O3*A20 (DNA-Chain B)	2.68
	[Cu(L-arg)(dpq)Cl]Cl (**4**)	
H(N5) (ligand)	O5*(T) (DNA-Chain A)	2.58
H(N7) (ligand)	O1(A) (DNA-Chain A)	2.47
H(N9) (ligand)	O1(A) (DNA-Chain A)	2.88
	[Cu(L-arg)(dppz)Cl]Cl (**5**)	
H(N13) (ligand)	O4(T) (DNA-Chain B)	3.05
H(N6)(A)(DNA-Chain A)	O6 (ligand)	2.57

[a] Donor group is Z and acceptor group is Y in the hydrogen bond (Y−H···Z).

The optimal binding conformation of **1** and **3** in the AT stretches of the minor groove forms an extensive H-bonding network with the A and T base pairs of B-DNA. This establishes that crescent-shaped backbone structure of the molecule that is important for efficient binding with the DNA in the minor groove. Complex **3** also shows favorable H-bonding interactions with the AT base pair sequences of ds-DNA and the positively charged guanidinium end group (2.7−3.0 Å). In addition, phen has a favorable stacking interaction with the DNA base pairs (Figure 6b; Figure S4a, Supporting Information). After observing the preferential AT selectivity of complexes **1** and **3**, we have carried out similar docking calculations for the dpq (**4**) and dppz (**5**) complexes with short-chain oligonucleotide poly(dA·dT)$_6$. Optimized energy-minimized structures of complexes **4** and **5** have been generated using the atomic coordinates of **3**. The docking results show the binding of **4** and **5** to the phosphate backbone of the polynucleotide involving the terminal positively charged guanidinium end groups of L-arginine through H bonding (2.8−3.0 Å) and ionic contacts along with favorable stacking interactions with the DNA base pairs (Figure 6c,d; Figure S4b,c, Supporting Information).

DNA Cleavage Properties. Chemical Nuclease Activity. The chemical nuclease activity of the copper(II) complexes has been studied under physiological conditions using agarose gel electrophoresis using supercoiled pUC19 DNA in a 50 mM Tris-HCl/50 mM NaCl buffer (pH 7.2) in the presence of MPA as a reducing agent. The DNA cleavage activity follows the order **5** (L-arg-Cu-dppz) ≥ **4** (L-arg-Cu-dpq) > **3** (L-arg-Cu-phen) > **1** (bis-L-arg-Cu) ≫ **2** (L-arg-Cu-bpy). Netropsin is found to be chemical-nuclease-inactive. A 5 μM solution of **4** and **5** essentially completely cleaves SC DNA to its nicked circular form (84% and 92%), while **3** shows only ∼60% conversion to the NC form (Figure 7). The bpy complex (**2**) is a poor DNA binder and cleaver. Control experiments using MPA or the complexes alone do not show any apparent cleavage of SC DNA. To determine the groove selectivity of the complexes, control experiments have been performed using minor-groove-binder distamycin. The phen and dpq complexes are found to be minor groove binders, as distamycin addition causes significant inhibition of DNA cleavage. The dppz complex does not show any inhibitory effect of distamycin but exhibits inhibition by methyl green, suggesting its major groove binding preference. Experiments have also shown that hydroxyl radical scavengers like DMSO, KI, or catalase inhibit the chemical nuclease activity. There is, however, no apparent inhibitory effect of SOD, suggesting the noninvolvement of $O_2^{\bullet-}$ in the cleavage reaction. Mechanistic data indicate the formation of a hydroxyl radical or copper-oxo species as the cleavage active species (Figure 8). The pathways involved in the DNA cleavage are believed to be similar to those proposed by Sigman and co-workers for the "chemical nuclease" activity of bis(phen)copper species.[73,74]

Photoinduced DNA Cleavage Activity. The DNA cleavage activity of netropsin and the complexes has been studied using SC pUC19 DNA (30 μM, 0.2 μg) in UV-A light of 365 nm and visible light of 647.1 nm (Ar−Kr CW mixed gas-ion laser) using a 10−50 μM concentration of the complexes in the absence of any external additives in a medium of Tris-HCl/NaCl buffer (50 mM, pH 7.2). The gel electrophoresis diagrams show the extent of DNA cleavage by the complexes (Figures 9−11). Selected cleavage data are given in Table 5. The bpy complex does not show any photoinduced DNA cleavage activity at 365 nm. Netropsin is apparently cleavage-inactive in UV-A light, showing only ∼16% conversion of the SC form to the NC form (lane 6, Figure 9). A 50 μM solution of [Cu(L-arg)$_2$]$^{2+}$ (**1**) exhibits ∼90% cleavage of SC DNA at 365 nm for 1 h of exposure time with a significant quantity of linear DNA formation. A 10 μM solution of complexes **3**−**5** shows essentially complete cleavage of the SC DNA under similar conditions. In addition, complexes **4** and **5** exhibit significant formation of linear DNA from dsb on the complementary strands. Complexes **4** and **5** are found to be more active compared to **1**−**3** due to the dual photosensitizing ability of the metal-bound L-arginine and dpq or dppz ligands. The light-induced DNA cleavage is likely to involve the dpq/dppz ligand, having a quinoxaline/phenazine moiety with conjugated C=N bonds that could generate photoexcited $^3(n-\pi^*)$ or $^3(\pi-\pi^*)$ state(s) effecting DNA cleavage following an oxidative pathway in addition to the photoactive guanidinium moiety of the amino acid.[65] Observation of linear DNA formation is of potential importance in cellular applications. The cellular DNA repair mechanism does not work easily in repairing the linear DNA obtained from dsb.[75−77] Control experiments using the ternary copper(II) complexes under dark conditions or the α-amino acid or the heterocyclic bases dpq and dppz alone at 365 nm do not show any apparent

(72) Kopka, M. L.; Yoon, C.; Goodsell, D.; Pjura, P.; Dickerson, R. E. *J. Mol. Biol.* **1985**, *183*, 553.
(73) Zelenko, O.; Gallagher, J.; Sigman, D. S. *Angew. Chem., Int. Ed. Engl.* **1997**, *36*, 2776.
(74) Thederahn, T. B.; Kuwabara, M. D.; Larsen, T. A.; Sigman, D. S. *J. Am. Chem. Soc.* **1989**, *111*, 4941.

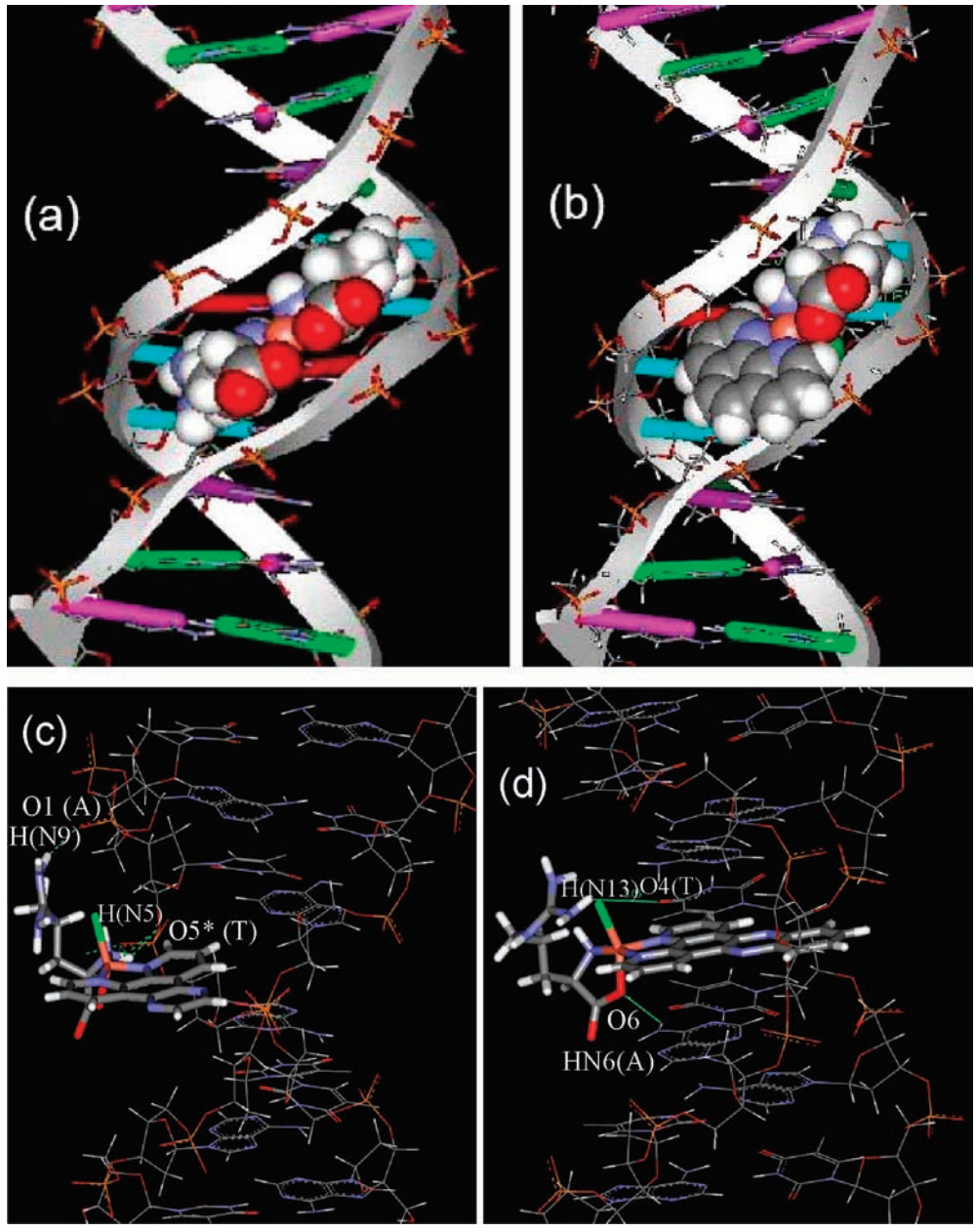

Figure 6. Views of the energy-minimized docked structure of $[Cu(L\text{-arg})_2]^{2+}$ (**1**) (a) and $[Cu(L\text{-arg})(phen)Cl]^{+}$ (**3**) (b) with $d(CGCGAATTCGCG)_2$. Views of the energy-minimized docked structure of $[Cu(L\text{-arg})(dpq)Cl]^{+}$ (**4**) (c) and $[Cu(L\text{-arg})(dppz)Cl]^{+}$ (**5**) (d) with $poly(dA\cdot dT)_6$ showing noncovalent interactions.

Figure 7. Gel electrophoresis diagram showing cleavage of SC pUC19 DNA (0.2 μg, 30 μM) by complexes **1**−**5** (5 μM) in the presence of 3-mercaptopropionic acid (MPA, 0.5 mM) in the dark: lane 1, DNA control; lane 2, DNA + **3**; lane 3, DNA + **1** + MPA; lane 4, DNA + **2** + MPA; lane 5, DNA + **3** + MPA; lane 6, DNA + **4** + MPA; lane 7, DNA + **5** + MPA; lane 8, DNA + distamycin (10 μM) + **3** + MPA; lane 9, DNA + distamycin (10 μM) + **4** + MPA; lane 10, DNA + distamycin (10 μM) + **5** + MPA; lane 11, DNA + methyl green (10 μM) + **5** + MPA.

cleavage of SC DNA. The amino acid L-arg in the metal-bound form, however, acts as a photosensitizer in visible light. The lack of any photocleavage activity of bpy complex **2** suggests the necessity of both the photoactive ligand and a good DNA binder in the ternary copper(II) structure for observing efficient photoinduced DNA cleavage activity. The better photocleavage activity of **3** than that of **1** could be related to their DNA binding propensities.

We have explored the photocleavage activity of the complexes in red light of 647.1 nm using a mixed gas-ion Ar−Kr CW laser (Figure 10). Netropsin is cleavage-inactive in red light. Binary complex **1** is also a poor cleaver of SC DNA in red light of 647.1 nm. In contrast, complex **3** shows ~60% conversion of the SC form to the NC form at this wavelength. The extent of DNA cleavage by the dpq (**4**) and

(75) Natrajan, A.; Hecht, S. M. *Molecular Aspects of Anticancer Drug-DNA Interactions*; Neidle, S., Waring, M., Eds.; CRC Press: Boca Raton, FL, 1994; Vol. *2*, p 197.
(76) Chen, J.; Stubbe, J. *Nat. Rev. Cancer.* **2005**, *5*, 102.
(77) Pamatong, F. V.; Detmer, C. A., III; Bocarsly, J. R. *J. Am. Chem. Soc.* **1996**, *118*, 5339.

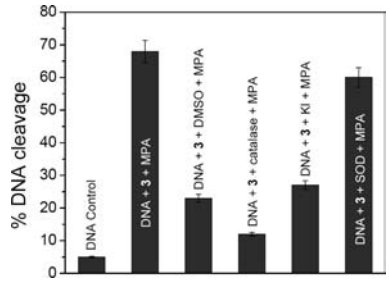

Figure 8. Bar diagram showing the cleavage of SC pUC19 DNA (0.2 μg, 30 μM) by **3** (5 μM) in the presence of MPA and different additives (DMSO, 4 μL; catalase, 4 units; KI, 10 μM; SOD, 4 units) in Tris-HCl/NaCl buffer (pH 7.2).

Figure 9. Gel electrophoresis diagram showing the photoinduced oxidative cleavage of SC pUC19 DNA (0.2 μg, 30 μM) by netropsin (ntp, 50 μM) and complexes **1**−**5** in 50 mM Tris-HCl/NaCl buffer (pH 7.2) on irradiation with UV-A light of 365 nm: lane 1, DNA control; lane 2, DNA + **3** (dark); lane 3, DNA + dpq (5 μM); lane 4, DNA + L-arg (50 μM); lane 5, DNA + $CuCl_2 \cdot 2H_2O$ (50 μM); lane 6, DNA + ntp (50 μM); lane 7, DNA + **1** (50 μM); lane 8, DNA + **2** (10 μM); lane 9, DNA + **3** (10 μM); lane 10, DNA + **4** (10 μM); lane 11, DNA + **5** (10 μM).

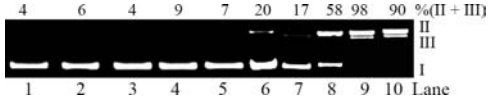

Figure 10. Red-light-induced cleavage of SC pUC19 DNA (0.2 μg, 30 μM) by netropsin (ntp, 50 μM) and complexes **1**−**5** in a 50 mM Tris-HCl/NaCl buffer (pH 7.2) using a 647.1 nm Ar−Kr CW laser (100 mW) for 1 h exposure time: lane 1, DNA control; lane 2, DNA + L-arg (50 μM); lane 3, DNA + $CuCl_2 \cdot 2H_2O$ (50 μM); lane 4, DNA + dpq (10 μM); lane 5, DNA + ntp (50 μM); lane 6, DNA + **1** (50 μM); lane 7, DNA + **2** (50 μM); lane 8, DNA + **3** (50 μM); lane 9, DNA + **4** (10 μM); lane 10, DNA + **5** (10 μM).

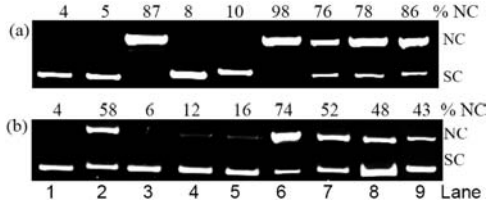

Figure 11. (a) Gel electrophoresis diagram showing the cleavage of SC pUC19 DNA (0.2 μg, 30 μM) by complex **1** (50 μM) using UV-A radiation of 365 nm (6 W) for 1 h exposure time in a 50 mM Tris-HCl/NaCl buffer (pH, 7.2): lane 1, DNA control; lane 2, DNA + **1** (dark); lane 3, DNA + **1**; lane 4, DNA + **1** (under argon); lane 5, DNA + NaN_3 (100 μM) + **1**; lane 6, DNA + D_2O (16 μL) + **1**; lane 7, DNA + DMSO (2 μL) + **1**; lane 8, DNA + catalase (4 units) + **1**; lane 9, DNA + SOD (4 units) + **1**. (b) Gel electrophoresis diagram showing photoinduced cleavage of SC pUC19 DNA (0.2 μg, 30 μM) by **3** (50 μM) at 674.1 nm laser wavelength for 1 h exposure time: lane 1, DNA control; lane 2, DNA + **3**; lane 3, DNA + $[Cu(phen)_2(H_2O)]^{2+}$ (50 μM); lane 4, DNA + **3** (under argon); lane 5, DNA + NaN_3 (100 μM) + **3**; lane 6, DNA + D_2O (16 μL) + **3**; lane 7, DNA + DMSO (4 μL) + **3**; lane 8, DNA + catalase (4 units) + **3**; lane 9, DNA + SOD (4 units) + **3**.

dppz (**5**) complexes is significantly higher than that by the phen analogue. This is possibly due to the greater DNA binding and photosensitizing ability of the quinoxaline and phenazine moieties. Two photoactive ligands in **4** and **5** could lead to the formation of linear DNA by attacking two complementary DNA strands at close proximity. The phen complex (**3**) having one photosensitizer (L-arg) shows formation of only NC DNA. The DNA cleavage activity in red light is believed to be metal-assisted in nature, involving metal-centered electronic band(s) in the photosensitization process, since the ligands individually do not have any absorption band at this wavelength. The ligands alone are cleavage-inactive in visible light. The positive role of the metal center is clearly evidenced since the organic amino acid conjugates with photoactive DNA binders are known to be photoinactive within the PDT window.[42−44]

Mechanistic aspects of the photoinduced DNA cleavage reactions are investigated in the presence of various additives in UV-A and red light (Figure 11). The complexes are cleavage-inactive at 365 nm in an argon atmosphere, indicating the necessity of molecular oxygen for the photocleavage of DNA. The addition of singlet oxygen quenchers like sodium azide or L-histidine significantly inhibits the DNA cleavage activity of the complexes. Involvement of $^1O_2$ is also indicated from the enhancement of DNA cleavage activity in D_2O, the solvent that shows a longer lifetime of $^1O_2$ compared to H_2O.[78] Hydroxyl radical scavengers such as DMSO or catalase have no apparent effect on the DNA photocleavage activity. Superoxide radical scavenger SOD does not show any inhibitory effect, suggesting noninvolvement of the $O_2^{\bullet -}$ in the photocleavage reaction. Control experiment data unequivocally suggest the involvement of singlet oxygen ($^1O_2$) as the reactive species in the photocleavage reaction in both UV-A and red light (Figure 12).[13,79] In summary, the photosensitizing effect of the {(L-arg)Cu(II)} moiety is observed in phen complex **3**, in which the photoinactive phen acts as a DNA minor groove binder and the amino acid L-arg with its cationic guanidinium moiety is a photosensitizer. A comparison of the photoinduced DNA cleavage activity of ternary amino acid copper(II) complexes shows that the photosensitizing effect of L-arginine is more than that of L-methionine but less than that of L-lysine.[32−34] The DNA binder heterocyclic bases dpq and dppz with their photoactivatable quinoxaline/phenazine moieties show a significant photosensitization effect, enhancing the overall cleavage activity of complexes **4** and **5** along with the formation of linear DNA.

Conclusions

We have prepared a binary complex $[Cu(L\text{-}arg)_2](NO_3)_2$ and a series of ternary copper(II) complexes [Cu(L-arg)-(B)Cl]Cl containing bidentate α-amino acid L-arginine and *N*,*N*-donor heterocyclic bases as models for natural antibiotic netropsin. Like netropsin, which shows shape complementarity in its AT-selective DNA minor groove binding, we have designed the copper(II)-based synthetic models of netropsin to probe their AT-selective DNA binding and, in addition, DNA photocleavage activity. The complexes display efficient DNA groove binding propensity and photoinduced DNA cleavage activity on irradiation with UV-A and red light. The binary copper(II) complex mimics the

(78) Khan, A. U. *J. Phys. Chem.* **1976**, *80*, 2219.
(79) Dhar, S.; Senapati, D.; Das, P. K.; Chattopadhyay, P.; Nethaji, M.; Chakravarty, A. R. *J. Am. Chem. Soc.* **2003**, *125*, 12118.

Table 5. Photoinduced pUC19 SC DNA (0.2 μg, 30 μM) Cleavage Data for Complexes **1**−**5** at 365 and 647.1 nm

sl. no.	reaction condition[a]	[complex]/μM: 365 nm [647.1 nm]	%NC DNA: 365 nm [647.1 nm]	%linear DNA: 365 nm [647.1 nm]
	Light Source: UV-A Light (365 nm, 6 W) [Ar−Kr CW Laser (647.1 nm, 100 mW)][b]			
1.	DNA control		3 [4]	
2.	DNA + [Cu(L-arg)(phen)Cl]Cl (**3**) (in dark)	10	4	
3.	DNA + ntp	50 [50]	16 [7]	
4.	DNA + $[Cu(L\text{-}arg)_2](NO_3)_2$ (**1**)	50 [50]	54 [20]	35
5.	DNA + [Cu(L-arg)(bpy)Cl]Cl (**2**)	10 [50]	18 [17]	
6.	DNA + [Cu(L-arg)(phen)Cl]Cl (**3**)	10 [50]	83 [58]	10
7.	DNA + [Cu(L-arg)(dpq)Cl]Cl (**4**)	5 [10]	52 [65]	45 [33]
8.	DNA + [Cu(L-arg)(dppz)Cl]Cl(**5**)	5 [10]	48 [68]	42 [22]

[a] Photoexposure time (t) = 1 h. SC and NC are supercoiled and nicked circular forms of pUC19 DNA, respectively. The error in measuring %DNA was ~3−5%. [b] Additional data on ligands (5 μM) and $CuCl_2 \cdot 2H_2O$ (50 μM) alone (%NC for 1 h photoexposure at 365 nm): dpq, 8; dppz, 6; L-arg (50 μM), 3 and $CuCl_2 \cdot 2H_2O$, 4.

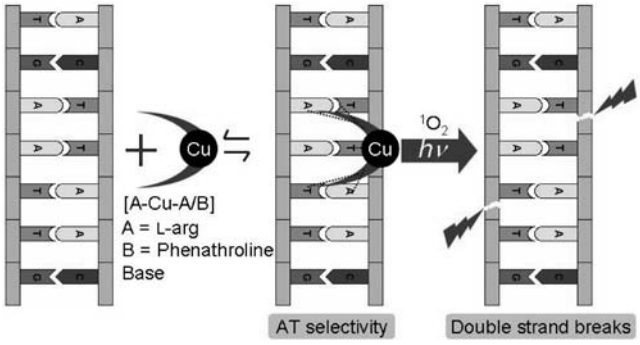

Figure 12. Schematic representation showing the AT-selective DNA binding and the proposed mechanism for the photoinduced DNA cleavage reaction of the complexes.

structural and AT-selective DNA binding properties of netropsin. It displays photoinduced DNA cleavage activity in red light, while netropsin is photoinactive in visible light. The oxidative photocleavage of DNA in the PDT window occurs in a metal-assisted photosensitization process involving the d−d band forming singlet oxygen as the reactive species.[79] The planarity and extended conjugation of the phenanthroline bases have a significant effect on the DNA binding and cleavage activity of complexes **3**−**5**. A mechanistic study shows a minor groove binding nature of the copper(II) bis arginate, phen, and dpq complexes, while the dppz complex binds at the major groove. The significant results include our observation of biologically important photoinduced DNA double-strand breaks leading to linear DNA formation due to the photosensitizing effect of both L-arg and dpq/dppz. The results are rationalized from DNA docking calculations showing noncovalent interactions of the complexes to the complementary DNA strands, making them susceptible to dsb. The results are of significance, as highly specific cell-permeable metal-based natural antibiotic analogues/mimics derived from 3d metal complexes with bioessential metal and photoactive α-amino acid/peptides showing red light-induced DNA cleavage activity could be tailored for potential cellular applications in PDT.

Acknowledgment. We thank the Department of Science and Technology (DST), Government of India, for financial support (SR/S1/IC-10/2004 and SR/S5/MBD-02/2007) and for the CCD single-crystal X-ray diffractometer facility. We also thank the Department of Biotechnology (DBT) for funding and the Alexander von Humboldt Foundation, Germany, for the donation of an electroanalytical system. A.K.P., T.B., and S.R. are thankful to CSIR, New Delhi, for research fellowships. A.R.C. thanks DST for J. C. Bose national fellowship.

Supporting Information Available: Cyclic voltammograms (Figure S1); unit cell packing diagram (Figure S2); energy-minimized docked structures showing noncovalent interactions (Figures S3, S4); selected bonding parameters for complex **3**·$2.5H_2O$ (Table S1); and crystallographic details in CIF format listing full crystallographic data, atomic coordinates, bond distances and bond angles, anisotropic thermal parameters, and the hydrogen-bonding coordinates for complex **3**·$2.5H_2O$ (CIF). This material is available free of charge via the Internet at http://pubs.acs.org.

IC8017425